ELSEVIER

Applied Surface Science 191 (2002) 128–137

applied surface science

www.elsevier.com/locate/apsusc

An X-ray photoelectron spectroscopic study of electrochemically deposited Fe–P thin films on copper substrate

C.L. Aravinda[a], Parthasarathi Bera[b], V. Jayaram[b], S.M. Mayanna[a,*]

[a]*Department of Chemistry, Central College, Bangalore University, Bangalore 560 001, Karnataka, India*
[b]*Solid State and Structural Chemistry Unit, Indian Institute of Science, Bangalore 560 012, Karnataka, India*

Received 1 October 2001; accepted 7 February 2002

Abstract

Electrochemically deposited Fe–P magnetic thin film from acidic tartarate complex bath solution was characterized by X-ray photoelectron spectroscopy. As-prepared film contains both Fe^{3+}- and P^{5+}-like species, whereas the same film after 10 and 20 min sputtering shows peaks corresponding to Fe metal as well as $P^{\delta-}$ species along with P^{5+} species. The film after heat-treatment contains Fe^{3+} together with P^{5+} and $P^{\delta-}$ species, whereas heat-treated film after sputtering shows the presence of both Fe metal and Fe^{2+} species. There is an increase in $P^{\delta-}$ intensity on sputtering the heat-treated film.

Keywords: Electrodeposition; Fe–P thin film; Magnetic properties; X-ray diffraction; X-ray photoelectron spectroscopy

1. Introduction

Binary amorphous alloys of iron group metals find extensive applications in fabrication of microelectronic devices in general, high-density magnetic storage medium (ribbons, compact disks, etc.) and thin film heads in particular [1,2]. Recently, the subject has been reviewed by Djokic [3]. Among various metal–metalloid alloys of iron group metals, Fe–P permalloy thin films deserves special attention as a cost effective soft magnetic amorphous material [4].

Fe–P alloy films can be processed by electrochemical [5], electroless [6], metallurgical [7], mechanical [8] and sputtering [9] methods. However, electrochemical method is extensively used because it allows control over composition and microstructure of the coatings by using suitable plating conditions [10]. A few bath solutions containing complexing agents have been developed [11,12], wherein, internal stress and magnetic properties of the deposited Fe–P alloy film found to depend on the addition agents beside the plating conditions. The major setback of the electrochemical method is the inclusion of components like sulfur, oxides/hydroxides derived from the bath solution. The change in plating conditions may also lead to change in structural aspects of the deposit though they possess similar composition [9]. These factors affect the magnetic properties considerably, which are greatly dependent on the structural aspects and local atomic composition of the deposits [13,14].

Hence, it requires comprehensive understanding of preparation and characterization to get high quality Fe–P alloy films. One of the interesting problems is to find out whether the alloy forms amorphous or

* Corresponding author. Tel.: +91-080-3301726; fax: +91-080-3219295.
E-mail address: smm@eth.net (S.M. Mayanna).

0169-4332/02/$ – see front matter
PII: S0169-4332(02)00171-X

crystalline structure as the bulk metal itself is able to dissolve up to 25 at.% phosphorous without a detectable second phase [15]. Here, we report the analysis of atomic compositions, effect of sputtering and inclusions of as-prepared as well as heat-treated Fe–P electrodeposits obtained from complex bath solution using X-ray photoelectron spectroscopy (XPS) and X-ray diffraction techniques (XRD).

2. Experimental

All solutions were prepared using analytical reagent grade chemicals and doubly distilled water. Thin films were deposited electrochemically on copper foils (99.9%, $2 \times 5\,cm^2$ area) under potentiostatic conditions using a stainless steel (SS 316) auxiliary electrode and a calomel reference electrode. The pre-treatment of the electrode surface and other experimental procedures have been given elsewhere [16]. Fe–P thin films were deposited to a constant thickness (~1000 nm) from the bath solution containing different additives such as sodium potassium tartarate (SPT, $0.025\,M < x < 0.1\,M$), sodium hypophosphite (SHP, $0.5\,M < x < 0.1\,M$) along with ferrous sulfate (0.1 M) and boric acid (0.05 M). L-Ascorbic acid was used in trace concentration (0.005 M) to reduce Fe^{3+}–Fe^{2+} ion, if any, thereby preventing the precipitation and subsequent incorporation of ferric hydroxide into the deposit [17]. The optimized bath composition and operating conditions to get coherent, pore-free alloy films with permalloy composition ($Fe_{80}P_{20}$) are given in Table 1.

The compositions of the films were obtained using an atomic absorption spectrometer (Perkin Elmer PHI 590 A). The magnetic properties (coercivity (H_c) and saturation magnetization (M_s)) were obtained using a vibrating magnetometer (EG and G PAR 155). XRD patterns of as-prepared as well as heat-treated (450 °C, 5 h, 10^{-6} Torr) samples were obtained on a Siemens D5005 X-ray diffractometer using Cu Kα radiation with Ni filter. XPS of the deposited thin films were recorded on an ESCA-3 Mark II spectrometer (VG Scientific, UK) using Al Kα radiation (1486.6 eV). The binding energies were measured with respect to C(1s) peak at 285 eV with a precision of ±0.2 eV. For XPS analysis the samples were placed into an ultra-high vacuum (UHV) chamber at 10^{-9} Torr housing the analyzer. Prior to mounting, the samples were kept in the preparation chamber at ultra-high vacuum (10^{-9} Torr) for 5 h in order to desorb any volatile species present on the surface. Intermittent sputtering was performed by using defocused Ar^+ ion beam with low voltage and low current over an area of $0.8 \times 2.4\,mm^2$. During sputtering of deposit a few angstrom of successive layer is removed and the composition of the material in the particular layer is investigated. The experimental data were curve fitted with Gaussian peaks after subtracting a linear background. For Gaussian peaks, slightly different full width at half maximum (FWHM) was used for different chemical states. The spin orbit splitting and the doublet intensities were fixed as given in the literature [18]. The concentrations of different chemical states were evaluated from the area of the respective Gaussian peaks.

3. Results and discussion

The hysteresis loops (Fig. 1) were obtained for as-deposited and heat-treated Fe–P thin films with different P content. The values of coercivity (H_c) and saturation magnetization (M_s) found to depend on the alloy composition (Table 2). Heat-treatment improves the magnetic properties of the alloy films. Alloy films

Table 1
Optimum bath composition and operating conditions to deposit $Fe_{80}P_{20}$ thin film

Composition	Concentration (M)	Operating conditions
$FeSO_4{\cdot}7H_2O$	0.1	pH: 3.0, temperature: 303 K, E_c: −1300 mV, time: 20 min, substrate: Cu foil, anode: SS316
$COOK(CHOH)_2COONa{\cdot}4H_2O$	0.1	
$NaH_2PO_2{\cdot}2H_2O$	0.05	
H_3BO_3	0.05	
$(OC)_2(OH)C(OHCH)_2CH_2OH$	0.005	

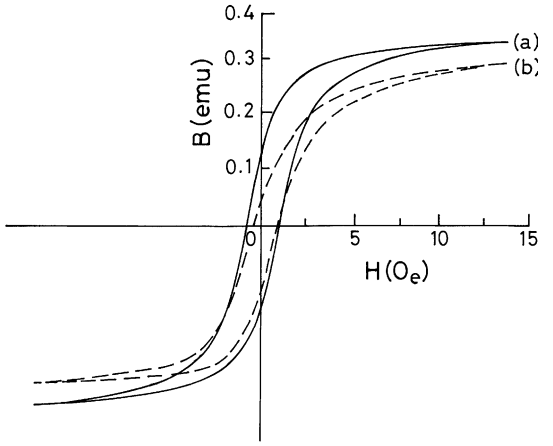

Fig. 1. Typical hysteresis loops of Fe–P film: (a) as-prepared (—) and (b) heat-treated (- - -).

with permalloy composition exhibiting good magnetic property were chosen for detailed investigations.

The typical XRD patterns of Fe–P thin films with and without heat-treatment are shown in Fig. 2. As-prepared film shows only broad Fe_α peak in the XRD pattern indicating the partial amorphous nature of the deposit. Peaks corresponding to Fe_3P and FeP_4 are observed along with Fe_α peak in the XRD pattern after heat-treatment, which indicates the formation of intermetallic phases upon heat-treatment.

Table 2
Dependence of magnetic properties on the composition of Fe–P alloy film[a]

P content (at.%)	Coercivity, H_c (Oe)[b]	Saturation magnetization, M_s (emu g^{-1})[b]	Squareness ratio
11	0.90 (0.8)	240 (210)	0.65 (0.75)
16	0.75 (0.6)	270 (230)	0.40 (0.50)
21	0.65 (0.5)	320 (280)	0.25 (0.03)

[a] $FeSO_4$: 0.1 M, SPT: 0.05 M, SHP: 0.2 M, H_3BO_3: 0.05 M, pH: 3.
[b] Values for heat-treated samples are given in parenthesis.

In Fig. 3, the Fe(2p) core level region XPS of as-prepared sample and the same after 10 min sputtering are shown. It is observed that Fe is in +3 oxidation state along with satellite peaks. Fe ($2p_{3/2,1/2}$) peaks at 711.0 and 724.0 eV (Fig. 3(a)) could be assigned to Fe^{3+} oxidation state [19]. Similarly, in the film after 10 min sputtering Fe(2p) peaks at 710.9 and 723.1 eV correspond to Fe^{3+} state only (Fig. 3(b)) are noticed. But the film after 20 min sputtering shows the peaks due to Fe metal as well as Fe^{3+} state along with satellite peaks (Fig. 4). Fe(2p) peaks could be deconvoluted

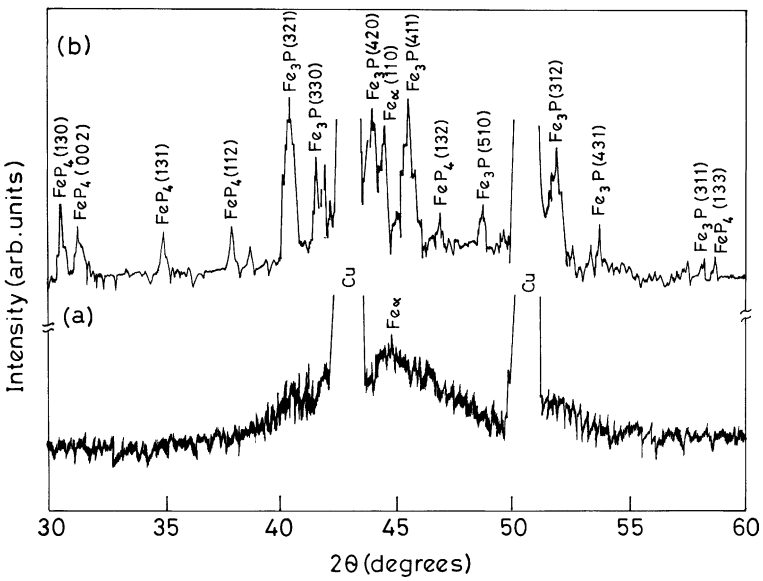

Fig. 2. XRD patterns of: (a) as-prepared and (b) heat-treated Fe–P film.

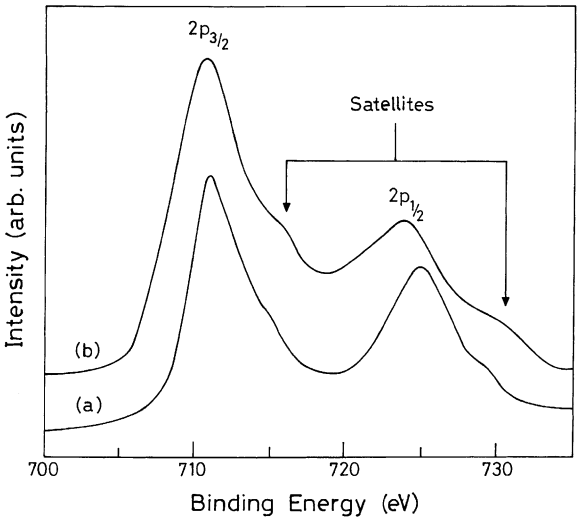

Fig. 3. XPS of Fe(2p) core level region of Fe–P thin film: (a) as-prepared and (b) after 10 min sputtering.

into sets of spin-orbit doublets. Accordingly, Fe($2p_{3/2}$) peaks at 707.8, 710.8 eV could be attributed to Fe^0 and Fe^{3+}, respectively [19]. Binding energies and relative intensities of different Fe species of as-prepared Fe–P film are given in Table 3.

In Fig. 5, Fe(2p) core level regions of heat-treated Fe–P film after (a) 10 and (b) 20 min sputtering are given. Heat-treated film shows Fe($2p_{3/2}$) peaks at 711.5 and 724.4 eV corresponding to Fe^{3+} state. In contrast, Fe(2p) spectrum of the heat-treated film after 10 and 20 min sputtering contains Fe($2p_{3/2}$) peaks at 707.4, 710.1, and 707.3, 710.1 eV, respectively. This indicates the presence of Fe^{2+} as well as Fe^0 in the sputtered film after heat-treatment (Fig. 5(a) and (b)). Binding energies and relative intensities of different Fe species of heat-treated Fe–P film are given in Table 4.

Table 3
Binding energies and relative intensities of different Fe species as observed from Fe(2p) spectra of as-prepared and sputtered Fe–P thin film

Sample	Species	Binding energy of $2p_{3/2}$ (eV)	Relative intensity (%)
As-prepared	Fe^{3+}	711.1	100
After 10 min sputtering	Fe^{3+}	710.9	100
After 20 min sputtering	Fe^0	707.8	40
	Fe^{3+}	710.8	60

XPS of P(2p) region of as-prepared film shows a peak at 133.2 which could be assigned to P^{5+} species since P(2p) peak in Na_2HPO_4 occurs at 133.1 eV [20]. P(2p) regions in film after (a) 10 and (b) 20 min sputtering are shown in Fig. 6. It is seen from the spectrum that P(2p) peaks occur at 129.6 and 133.0 eV. The higher binding energy peak can be ascribed due to P^{5+} species only. Binding energy for P(2p) level in red phosphorous is 130.2 eV [20].

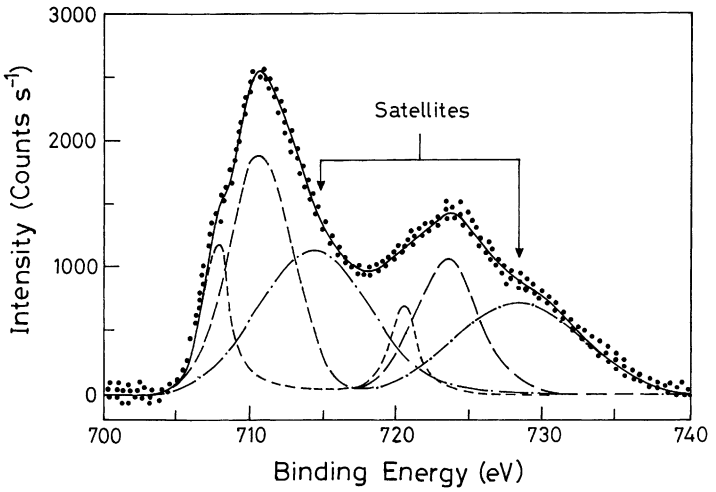

Fig. 4. XPS of Fe(2p) core level region of Fe–P film after 20 min sputtering.

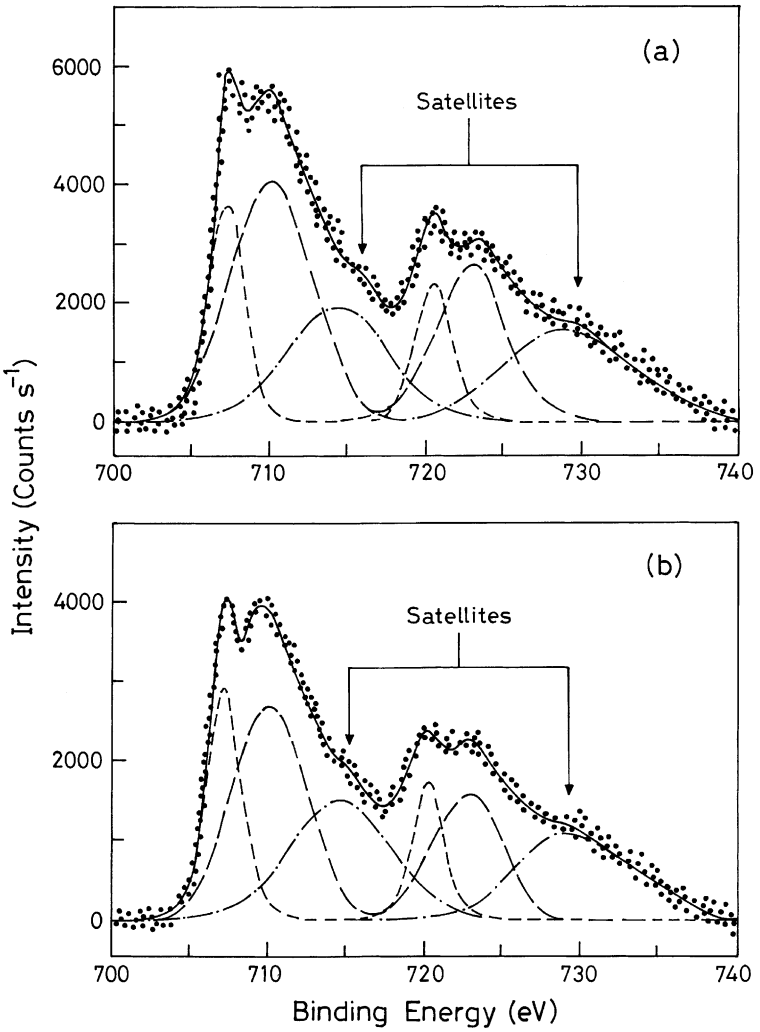

Fig. 5. XPS of Fe(2p) core level region of heat-treated Fe–P film: (a) after 10 min sputtering and (b) after 20 min sputtering.

Table 4
Binding energies and relative intensities of different Fe species as observed from Fe(2p) spectra of heat-treated Fe–P thin film

Sample	Species	Binding energy of $2p_{3/2}$ (eV)	Relative intensity (%)
Heat-treated	Fe^{3+}	711.5	100
After 10 min sputtering	Fe^{0}	707.4	47
	Fe^{2+}	710.1	53
After 20 min sputtering	Fe^{0}	707.3	52
	Fe^{2+}	710.1	48

Therefore, P(2p) peak in film is shifted by −0.6 eV with respect to P(2p) peak of red phosphorous. The direction of shift of 2p emission of P shows that it is in a negatively charged state ($P^{\delta-}$). XPS of P(2s) core level regions of as-prepared as well as after sputtering Fe–P film are shown in Fig. 7. Binding energy of P(2s) in phosphorous is 189.0 eV. Therefore, the shifted P(2s) peak at 191.0 eV indicates the presence of P^{5+} species in the sample. XPS spectra of P(2s) core level region of both 10 and 20 min sputtered film show two peaks at 187.5 and 191.1 eV (Fig. 7(b) and (c)) indicating the presence of $P^{\delta-}$ as well as P^{5+} species in the sputtered sample. Binding energies and relative

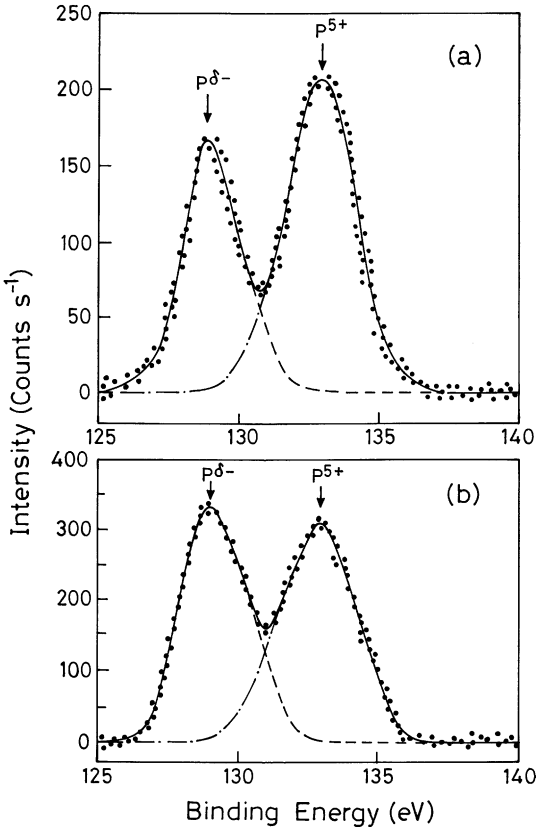

Fig. 6. XPS of P(2p) core level region of Fe–P film: (a) after 10 min sputtering and (b) after 20 min sputtering.

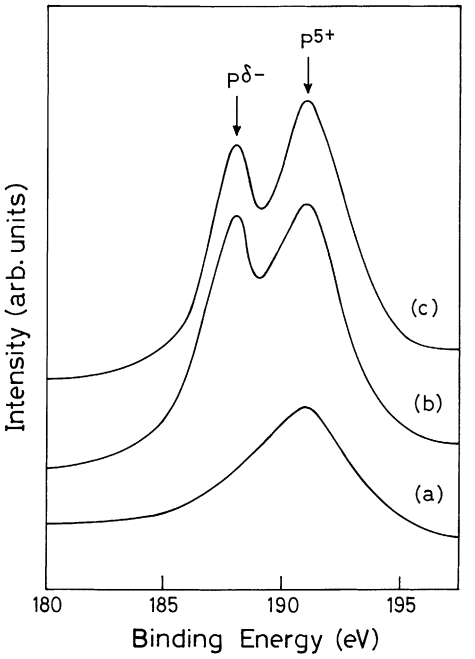

Fig. 7. XPS of P(2s) core level region of Fe–P film: (a) as-prepared, (b) after 10 min sputtering and (c) after 20 min sputtering.

intensities of P(2p) and P(2s) core levels of different P species in as-prepared Fe–P film are given in Table 5.

Heat-treated film shows two types of peaks at 129.6 and 133.3 eV in P(2p) region indicating the presence of $P^{\delta-}$ and P^{5+} species in the film. After 10 and 20 min sputtering of heat-treated film shows an increase in concentration of $P^{\delta-}$ species in comparison with P^{5+} species. XPS of P(2p) core level region of heat-treated film at different conditions are shown in Fig. 8. The P(2s) core level region spectra of heat-treated Fe–P film after (a) 10 and (b) 20 min sputtering are given in Fig. 9. Peak at 191.1 eV has been attributed to P^{5+} species, whereas peak at 187.7 eV can be due to the presence of $P^{\delta-}$ species in the film after heat-treatment. After 10 and 20 min sputtering there is an increase of $P^{\delta-}$ intensity compared to P^{5+}. Binding energies and relative intensities of P(2p) and P(2s) core levels of different P species in heat-treated Fe–P film are given in Table 6.

Table 5
Binding energies and relative intensities of different P species as observed from P(2p) and P(2s) spectra of as-prepared and sputtered Fe–P thin film

Sample	Species	Binding energy of 2p (eV)	Relative intensity (%)	Binding energy of 2s (eV)	Relative intensity (%)
As-prepared	P^{5+}	133.2	100	191.1	100
After 10 min sputtering	P^{5+}	133.0	53	191.0	49
	$P^{\delta-}$	129.6	47	187.7	51
After 20 min sputtering	P^{5+}	133.1	49	191.2	48
	$P^{\delta-}$	129.7	51	187.5	52

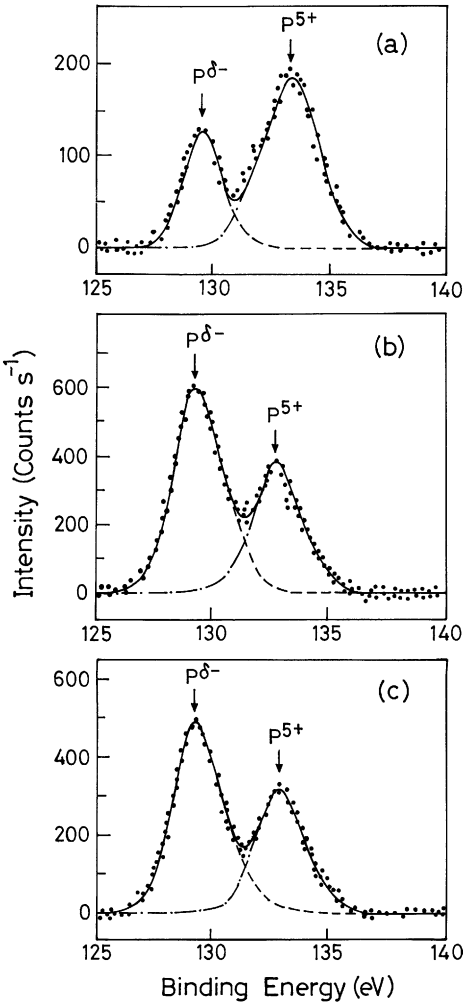

Fig. 8. XPS of P(2p) core level region of heat-treated Fe–P film: (a) after heat-treatment, (b) after 10 min sputtering and (c) after 20 min sputtering.

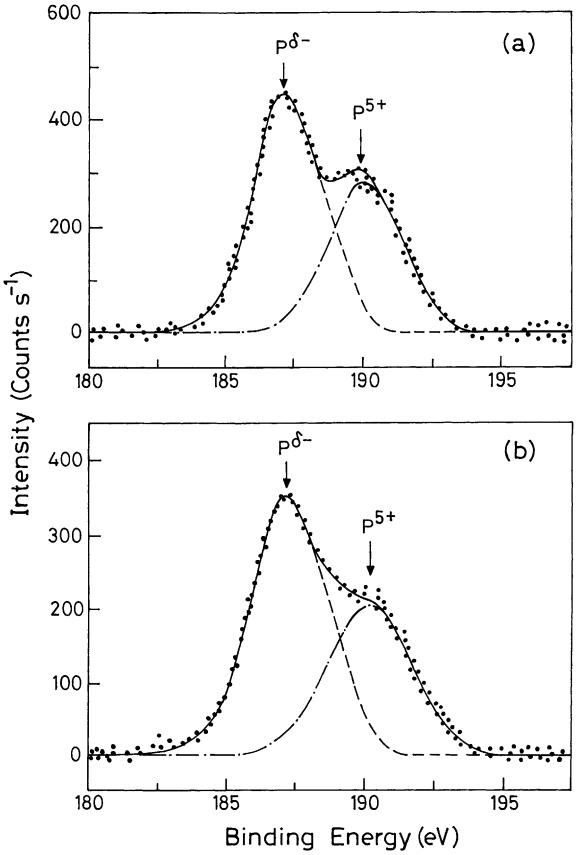

Fig. 9. XPS of P(2s) core level region of heat-treated Fe–P film: (a) after 10 min sputtering and (b) after 20 min sputtering.

XPS of O(1s) core level region in as-prepared, after 10 and 20 min sputtering are given in Fig. 10. The spectra could be deconvoluted into three components labeled as 1–3. O(1s) spectrum in as-prepared film shows intense peak at 532.1 eV along with a weak peak at 530.0 eV. The lower binding energy peak at

Table 6
Binding energies and relative intensities of different P species as observed from P(2p) and P(2s) spectra of heat-treated Fe–P thin film

Sample	Species	Binding energy of 2p (eV)	Relative intensity (%)	Binding energy of 2s (eV)	Relative intensity (%)
Heat-treated	P^{5+}	133.3	60	191.0	56
	$P^{\delta-}$	129.6	40	187.5	44
After 10 min sputtering	P^{5+}	133.1	40	191.2	39
	$P^{\delta-}$	129.6	60	187.4	61
After 20 min sputtering	P^{5+}	133.2	39	191.1	37
	$P^{\delta-}$	129.5	61	187.7	63

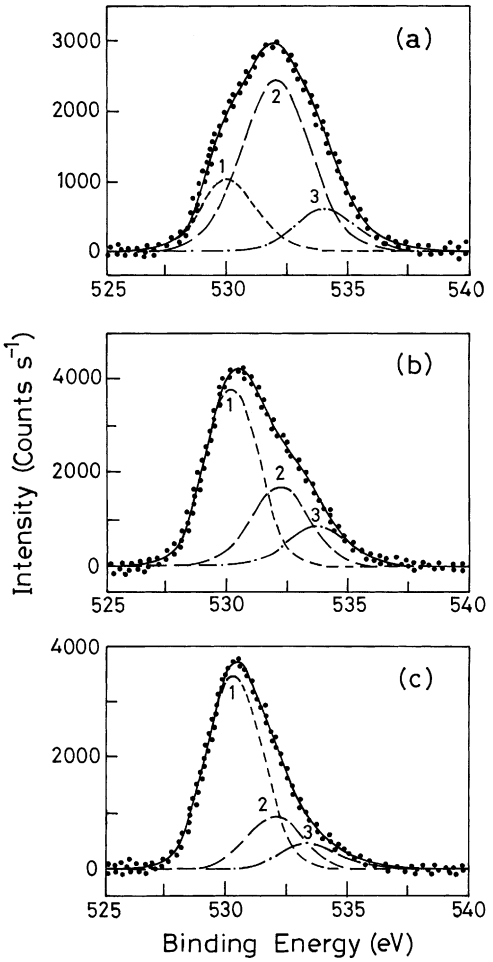

Fig. 10. XPS of O(1s) core level region of Fe–P film: (a) as-prepared, (b) after 10 min sputtering and (c) after 20 min sputtering.

530.0 eV could be attributed to O^{2-} type of species associated with oxides of iron, whereas P^{5+} species are responsible for the higher binding energy peak at 532.1 eV [20]. A comparison of the relative intensities of the two O(1s) peaks shows that the amount of oxygen associated with P is more than that associated with Fe. Taking this fact together with the observation that as-prepared film always contains P^{5+} and most probable species for the higher binding energy O(1s) peak is phosphate (PO_4^{3-}). The intensity of the peak at 532.1 eV decreases after 10 and 20 min sputtering and accordingly, lower binding energy peak intensity increases. This indicates that O^{2-} type of species

Table 7
Binding energies and relative intensities of different oxygen species as observed from O(1s) spectra of as-prepared film

Sample	Species	Binding energy of 1s (eV)	Relative intensity (%)
As-prepared	1	530.0	26
	2	532.1	59
	3	533.9	15
After 10 min sputtering	1	530.1	60
	2	532.2	27
	3	533.8	13
After 20 min sputtering	1	530.3	70
	2	531.9	20
	3	533.6	10

predominate in the sputtered film compared to oxygen associated with phosphorous suggesting the reduction of PO_4^{3-} to $P^{\delta-}$. A weak peak at 533.9 eV in all the figures indicates the presence of H_2O component in the sample from the complex bath solution while it decreases on sputtering. Binding energies and relative intensities of O(1s) peaks in as-prepared film is given in Table 7. On the other hand, intensities of O^{2-} species in heat-treated film at different conditions are less compared to as-prepared film.

The surface concentration ratio of Fe(2p)–P(2p) can be evaluated by the relation:

$$\frac{C_{Fe}}{C_P} = \frac{I_{Fe}\sigma_P\lambda_P D_E(P)}{I_P\sigma_{Fe}\lambda_{Fe}D_E(Fe)}$$

where C, I, σ, λ and D_E are the concentration, intensity, photoionization cross-section, electron attenuation length and geometric factor, respectively. Integrated intensities of Fe(2p) and P(2p) peaks have been taken into account for calculating the concentrations. Photoionization cross-sections and electron attenuation length have obtained from the literature [21,22]. The surface concentration ratios of Fe–P at different conditions are given in Table 8. The surface concentration ratio of Fe–P is 4.9 in as-deposited film suggesting the same surface concentrations of Fe and P for the surface and bulk. Hence, there is no segregation of either Fe or P in the as-deposited film. In contrast, the concentration ratio is 2.7 for heat-treated film indicating the increase in P concentration. This is due to the formation of $P^{\delta-}$ kind of species in heat-treated film in comparison with as-deposited film. On

Table 8
Surface concentration ratios of Fe(2p)–P(2p) in Fe–P film at different conditions

Sample	C_{Fe}/C_P[a]
As-prepared	4.9 (2.7)
10 min sputtering	3.1 (1.9)
20 min sputtering	1.6 (1.8)

[a] Values for heat-treated samples are given in parenthesis.

sputtering, P concentration increases in both as-deposited and heat-treated film.

Bath solution containing additives is employed here to get alloy deposits. The phosphorous content in the deposited films depends on the bath composition and deposition time. However, alloy electrodeposition being a complex process, it is very difficult to conclude the influence of a single parameter like pH, concentration and deposition time on the chemical composition of the deposit. Also, the variation of composition could reflect the properties of the deposits. From XPS studies it is clear that as-prepared as well as heat-treated film contains Fe^{3+} species. The decrease in intensity of Fe^{3+} species and appearance of metallic Fe on successive sputtering indicates that to some extent the deposit is prone to surface oxidation. Phosphorous is in +5 state in as-prepared film and P^{5+} and $P^{\delta-}$ species appear on sputtering. Reduction of phosphate to phosphide does not occur due to Ar^+ ion sputtering and therefore, removal of surface oxide layer leaves the alloy surface. On the other hand, phosphorous is in P^{5+} and $P^{\delta-}$ states in heat-treated film and the drastic increase in the concentration of $P^{\delta-}$ species compared to P^{5+} species upon successive sputtering indicates the variation in the concentration of different kinds of intermetallic compounds like Fe_3P and FeP_4 in the corresponding layer. There is no inclusion components of S (152 eV), Cl (181 eV) and Na (990 eV).

4. Conclusions

Fe–P permalloy films deposited from acidic tartarate bath exhibits good magnetic properties. Further, heat-treatment improves the magnetic properties of the alloy films. XRD studies show the formation of intermetallic phases in the Fe–P film upon thermal treatment. XPS study shows that Fe is in +3 state in both as-prepared and heat-treated Fe–P film. In as-prepared film after sputtering Fe metal as well as Fe^{3+} species have been observed and intensity of Fe metal increases. Film after heat-treatment shows Fe metal as well as Fe^{2+} on sputtering. Sputtering improves the intensity of $P^{\delta-}$-like species in the film. $P^{\delta-}$-like species predominates over P^{5+} species in heat-treated sample after sputtering. The surface concentration P increases in heat-treated as well as sputtered film due to the presence of $P^{\delta-}$ species. There are no inclusion components like S, Na, Cl in the as-prepared as well as heat-treated sample.

Acknowledgements

We thank Professor M.S. Hegde, Solid State and Structural Chemistry Unit, Indian Institute of Science, Bangalore for providing XPS facility and for useful discussion. The authors (CLA and SMM) are grateful to UGC, New Delhi for financial assistance to carry out this work.

References

[1] J. Lemke, MRS Bull. 15 (1990) 31.
[2] R. Hasegawa, J. Magn. Magn. Mater. 100 (1991) 1.
[3] S.S. Djokic, J. Electrochem. Soc. 146 (1999) 1824.
[4] K. Kamei, Y. Maehara, J. Appl. Electrochem. 26 (1996) 529.
[5] K. Kamei, Y. Maehara, Mater. Sci. Eng. A 181/182 (1994) 906.
[6] S.M. Mayanna, K. Raj, L. Ramesh, D. Landolt, Ciencia Tech. Dos Mater. 8 (1996) 38.
[7] K. Tanaka, N. Soga, K. Hirao, K. Kimura, J. Appl. Phys. 60 (1986) 728.
[8] E.P. Yelsukov, G.N. Konygin, A.V. Zagainov, V.A. Barinov, J. Magn. Magn. Mater. 195 (1999) 601.
[9] R.L. McCally, K. Moorjani, J. Appl. Phys. 67 (1990) 5784.
[10] C.L. Aravinda, S.M. Mayanna, Trans. IMF 77 (1999) 87.
[11] S. Vitkova, M. Kjuchukova, G. Raichevski, J. Appl. Electrochem. 18 (1988) 673.
[12] S. Armynov, S. Vitkova, O. Blajiev, J. Appl. Electrochem. 27 (1997) 185.
[13] F. Stein, G. Dietz, J. Magn. Magn. Mater. 117 (1992) 45.
[14] E.P. Elsukov, Y.N. Vorobev, A.V. Trubachev, Phys. Stat. Sol. (a) 127 (1991) 215.
[15] A. García-Arribas, M.L. Fdez-Gubieda, I. Orúe, J.M. Barandiarán, J. Herreros, F. Plazaola, Phys. Rev. B 52 (1995) 12805.
[16] T. Mimani, S.M. Mayanna, J. Electrochem. Soc. 140 (1993) 984.

[17] S.N. Srimathi, S.M. Mayanna, Mater. Chem. Phys. 11 (1984) 351.
[18] D. Briggs, M.P. Seah, Practical Surface Analysis by Auger and X-ray Photoelectron Spectroscopy, Wiley, New York, 1984, p. 503.
[19] A.M. Visco, F. Neri, G. Neri, A. Donato, C. Milone, S. Galvagno, Phys. Chem. Chem. Phys. 1 (1999) 2869.
[20] K.S. Rajam, S.R. Rajagopalan, M.S. Hegde, B. Viswanathan, Mater. Chem. Phys. 27 (1991) 141.
[21] J.H. Scofield, J. Electron. Spectrosc. Relat. Phenom. 8 (1976) 129.
[22] H. Ebel, C. Pöhn, R. Svagera, M.E. Wernle, M.F. Ebel, A. Jabłonski, J. Electron. Spectrosc. Relat. Phenom. 50 (1990) 109.